Cognition 264 (2025) 106259

Contents lists available at ScienceDirect

Cognition

journal homepage: www.elsevier.com/locate/cognit

Full Length Article

Spatiotemporal dynamics of mouse tracking reveal general and selective control mechanisms of the congruency sequence effect in Simon tasks

Minwoo J.B. Kim [a], Chae Eun Lim [b], Hansol Rheem [c], Nahyun Lee [d], Yang Seok Cho [d,*]

[a] Department of Biomedical Engineering, Ulsan National Institute of Science and Technology, South Korea
[b] Department of Cognitive, Linguistic & Psychological Sciences, Brown University, USA
[c] Department of Psychological Science, Kennesaw State University, USA
[d] School of Psychology, Korea University, South Korea

ARTICLE INFO

Keywords:
Simon task
Congruency sequence effect
Post-conflict slowing
Cognitive control
Mouse tracking

ABSTRACT

Competition between conflicting responses enhances cognitive control over responses on the subsequent trial, generating a congruency sequence effect (CSE). The present study investigated the mechanism of post-conflict control involved in the CSE by measuring the spatiotemporal dynamics underlying the Simon task with computer-mouse tracking. To examine control-specific CSEs driven by response conflict, a confound-minimized design was employed, rigorously controlling for stimulus repetitions, response repetitions, contingency learning, and response errors. We presented horizontal and vertical Simon tasks, each with two distinct stimulus and response alternatives, in a trial-to-trial interchanging order. Participants responded by moving a mouse cursor from the screen center to a target response box, determined by stimulus color rather than its location. Dynamic features of spatial precision and movement speed, as well as discrete movement latency and spatial features, were analyzed. Beyond the typical Simon effect, we identified post-conflict slowing and selective suppression of task-irrelevant response activation as two distinguishable modes of post-conflict control that manifest in different movement features and processing stages. This suggests that the CSE likely arises from two sub-processes of post-conflict control, rather than a unitary mechanism.

1. Introduction

Cognitive control flexibly adapts behavior according to current task goals. When faced with multiple competing manual responses, performance is controlled by adjusting the relative strength and timing of the co-activated responses. In Simon (Simon & Rudell, 1967), Stroop (Stroop, 1935), and flanker-compatibility tasks (Eriksen & Eriksen, 1974), the latency difference between the trials with (incongruent) and without (congruent) response conflict is called the congruency effect that quantifies the magnitude of response conflict. The congruency effect can be further reduced by response conflicts from preceding incongruent trials (Gratton, Coles, & Donchin, 1992) and such sequential modulation is known as the *congruency sequence effect* (CSE).

An extensive number of studies have identified two independent mechanisms behind the CSE. One major contributor is cognitive control or *conflict adaptation* in which the brain circuit for conflict monitoring situated at the anterior cingulate cortex regulates motor responses upon detection of response conflicts (Botvinick, Braver, Barch, Carter, & Cohen, 2001; Gratton et al., 1992). Another is priming from repetitive stimulus features and response modes that generates similar RT patterns to the control mechanism (Hommel, Proctor, & Vu, 2004; Mayr, Awh, & Laurey, 2003). Still, prominent CSEs continued to be observed in conflict tasks without stimulus or response repetitions suggesting that cognitive control is an independent source of action control (Lee & Cho, 2013; Lim & Cho, 2021b; Notebaert, Gevers, Verbruggen, & Liefooghe, 2006).

Yet the characteristics of the control mechanism behind the CSE are still debated. The conflict adaptation account suggested a unitary control mechanism in which a previous incongruent trial enhances control improving performance for upcoming trials (Gratton et al., 1992). Interestingly, performance cost typically occurs in congruent trials following incongruent trials (iC vs. cC trials). The performance cost is considered evidence of the control mechanism that operates through selective *suppression of task-irrelevant response* activations (e.g., Hübner & Mishra, 2013; Kim, Lee, & Cho, 2015; Y. S. Lee & Cho, 2023; Lee & Sewell, 2024; Stürmer, Leuthold, Soetens, Schröter, & Sommer, 2002; Ridderinkhof, 2002; Soutschek, Müller, & Schubert, 2013). This is

* Corresponding author.
E-mail address: yscho_psych@korea.ac.kr (Y.S. Cho).

https://doi.org/10.1016/j.cognition.2025.106259
Received 16 January 2025; Received in revised form 6 July 2025; Accepted 14 July 2025
Available online 17 July 2025

because suppression of congruent task-irrelevant information no longer aids correct response activations. An alternative account suggested that the control specific CSE is caused by the *amplification* of the task-relevant stimulus features following a previous response conflict (Egner & Hirsch, 2005; Scherbaum, Frisch, Dshemuchadse, Rudolf, & Fischer, 2018) but amplification did not successfully address the performance cost in iC trials. Whether control occurs through suppression or amplification is still actively debated, but recent reconciliatory views propose that suppression and amplification are optimal control strategies for different types of conflicts (see Braem, Abrahamse, Duthoo, & Notebaert, 2014 and Egner, 2008, 2014 for reviews).

Meanwhile, recent studies have raised skepticism over a single mechanism responsible for control and proposed a dual-mechanism account in which incongruent trials generate a domain-general *post-conflict slowing* effect together with selective control (e.g., Erb, McBride, & Marcovitch, 2019; Verguts, Notebaert, Kunde, & Wühr, 2011). Post-conflict slowing is similar to post-error slowing that is mediated by the inferior frontal junction (King, Korb, von Cramon, & Ullsperger, 2010). They are similar in the sense that the response criteria shifts sacrificing speed for better accuracy but can occur with response conflicts without explicit errors (Botvinick et al., 2001; Guan & Wessel, 2022; Heuer & Wühr, 2025; King et al., 2010; Rey-Mermet & Meier, 2017a, 2017b; Ridderinkhof, 2002; Verguts et al., 2011). Previous evidence suggested that post-conflict slowing is prevalent during the CSE by using univalent probes that do not trigger a response conflict following a previous response conflcit within that trial. In such cases, previous conflicts simply delayed responses rather than facilitating responses which explains the performance cost typically observed in iC vs. cC trials of the CSE (Verguts et al., 2011). However, post-conflict slowing has been overlooked because facilitation from selective control masks the response delay in consecutive response conflict trials (iI vs. cI). Recent studies further confirm the presence of domain-general post-conflict slowing in typical Simon tasks with minimized repetition confounds. Studies using key-release and directed responses show that post-conflict slowing is localized to the early stage of response when response time was divided into response initiation time (IT) and movement time (MT) (N. Lee & Cho, 2024; Y. S. Lee & Cho, 2023; Lim & Cho, 2021b), especially when all responses were made within the same hand (Lim & Cho, 2021b; exp. 1). The facilitation in the iI vs. cI trials caused by selective control was reflected in the MT stage, showing evidence of a dual-mechanism of the CSE.

Still, latency measures are indirect measures of response conflict since latency can be influenced by the magnitude of response conflict, response onset delays, as well as dynamic changes in response execution speed. Alternatively, limb tracking methods have highlighted the underlying spatiotemporal dynamics of the latency measures across various fields of study and in the context of cognitive control (e.g., Buetti & Kerzel, 2008; Calderon, Gevers, & Verguts, 2018; Dale, Kehoe, & Spivey, 2007; Dieciuc, Roque, & Boot, 2019; Erb & Marcovitch, 2018; Erb, Moher, Sobel, & Song, 2016; Hehman, Stolier, & Freeman, 2015; Kim, 2024; Mittelstädt, Leuthold, & Mackenzie, 2023; Rheem, Vaughn Becker, & Craig, 2021; Salzer & Friedman, 2020; Scherbaum, Dshemuchadse, & Kalis, 2008; Song & Nakayama, 2009; Spivey, Grosjean, & Knoblich, 2005). For example, Scherbaum, Dshemuchadse, Fischer, and Goschke (2010); Scherbaum et al. (2018) investigated the CSE by measuring limb movements using the mouse (i.e., input device) during an arrow Simon task. They showed robust sequential modulations in the spatial features of the mouse movements, although their main focus was not on measuring post-conflict slowing. Several studies using hand reaching within Stroop (Erb et al., 2016; Erb & Marcovitch, 2019), flanker (Erb et al., 2016; Erb & Marcovitch, 2018; see Erb, Smith, & Moher, 2021 for review) and Simon tasks (Erb & Marcovitch, 2019) did specifically target post-conflict slowing and showed that post-conflict slowing is consistently reflected in the early movement initiation time (IT).

Meanwhile, the typical pattern of CSE was frequently observed in the MT latency and in the curvatures of the movement trajectory. Erb et al. (2016) found CSEs in MT and the movement curvature in a color-word Stroop task (Experiment 1). Erb and Marcovitch (2019) also observed a significant CSE in the curvatures and MT in a Simon task study across various age groups in trials without stimulus feature or response repetitions. In contrast, some studies failed to observe CSEs in the MT or the curvatures. Erb et al. (2016) showed that the CSE did not occurr in MT and curvatures in the letter flanker task in their Experiment 2 (e.g., AAKAA) when repetition trials were excluded, which contradicts results from *arrow* (e.g., >><>>) flanker studies (Erb & Marcovitch, 2018; Lim & Cho, 2021b).

The inconsistent findings of the CSE in MT and curvatures can partially attributed to how repetition priming was controlled. Previous mouse and hand-tracking studies compared trials with repeating stimulus/response sequences to non-repeating sequences (Erb & Marcovitch, 2019) or discarded feature repetition trials during analysis (e.g., Erb et al., 2016; Scherbaum et al., 2010, 2018). These strategies sacrifice statistical power by excluding a large number of trials (Schmidt & Weissman, 2014) and assume that the top-down control and bottom-up repetition priming mechanisms do not interact, which is not necessarily true (Lim & Cho, 2021a; Notebaert et al., 2006). Another method of controlling repetition priming is to use a four alternate forced choice (4AFC) response layout. This approach avoids partial repetitions by increasing the number of stimuli and response alternatives. However, using a 4AFC may introduce contingency learning as a novel confound: the proportion of incongruent trials may increase, and participants could learn to respond faster and more accurately to the more frequent incongruent trial types (for detail see Mordkoff, 2012 and Schmidt & De Houwer, 2011).

An optimal method is to use designs that constantly alternate between sets with non-overlapping stimuli and responses. Kim and Cho (2014) achieved this by presenting vertical and horizontal flanker-compatibility tasks with two distinct stimulus and response sets alternatingly in a trial-by-trial manner and still observing the CSE. Contingency learning was prevented by using two alternating 2AFC responses sets instead of a single 4AFC layout. This unique cross-task design was applied for various tasks including the Simon effect (Lim & Cho, 2021b). Between two alternating Simon tasks, the lingering influence from feature/response repetitions from N^{-2} trials is shown to have a trivial effect of the CSE between N^{-1} and N^{0} trials (Lim & Cho, 2021a). The alternating cross-task design is becoming increasingly recognized as an effective way to observe control-specific CSEs (Braem et al., 2014; Egner, 2014).

Currently, the spatiotemporal dynamics of the CSE in a confound minimized Simon task has not been examined. The current study uses the alternating cross-task design in combination with computer mouse movement measurements. Our aim is to confirm the existence of post-conflict slowing by providing detailed description of its spatiotemporal dynamics reflected in the spatial deviations, movement speed, and the latencies associated with control. The existence of domain-general slowing would indicate that at least two control mechanisms cooperate to improve action control in the future when experiencing response conflicts. Various movement features were derived from the trajectories, such as discrete movement latencies, discrete and dynamic spatial deviations, and dynamic movement speed. If post-conflict slowing were to be present, we expected to find a delay in movement initiation time (IT) and changes in early speed dynamics. As time progresses, the CSE would later occur in MT and in the spatial measurements (X_{min}, T_{length}, $X_{dynamic}$, and Angle) in response to the current trial congruency as a function of the previous trial congruency.

2. Methods

2.1. Transparency and openness

Power analysis for determining the sample size, the criteria, the

amount of excluded data, all experimental manipulations, all measurement methods, and procedures are reported in the manuscript following the TOP guidelines (Nosek et al., 2015). See the apparatus and stimuli section for the research materials. The data and analysis code for statistical analysis are available at [https://osf.io/5vpuw/]. The study design and its analysis were not pre-registered.

2.2. Participants

The current study recruited thirty students (14 men and 16 women, mean age = 23.75) from Korea University and took part in the experiment after giving written informed consent. According to our power analysis using MorePower6 (Campbell & Thompson, 2012) for a 2 by 2 repeated-measures ANOVA and an alpha level of 0.05, a sample of 30 was able to correctly detect significant effects sizes greater than 0.225 partial eta squared with less than 20 % of committing a type 2 error. Given the large effect sizes observed in the current study with a partial eta-squared value of 0.291 in MT, a sample of 30 were enough to obtain significant results with sufficient power. Bayes Factors are provided for further statistical rigor (see analysis section).

All participants had normal or corrected-to-normal visual acuity, had normal color vision, and were right-handed. KRW 7000 (about 6 US dollars) was offered to the participants as compensation at the end of the experiment. The current experiment was approved by the Institutional Review Board at Korea University (KUIRB-2020-0121-01).

2.3. Apparatus

Stimuli were presented with a 17-in. CRT monitor (1024 × 768 px; 32.3 × 23.3 cm), at a viewing distance of 60 cm. Responses were made via a standard computer mouse. The x and y coordinates of the computer mouse trajectories were recorded at the sampling rate of 100 Hz. All stimuli and responses were controlled by the mousetrap plug-in (Kieslich & Henninger, 2017), implemented in the experimental software OpenSesame (Mathôt, Schreij, & Theeuwes, 2012). MATLAB (2023b, Mathworks, MA), Python (3.9, van Rossum, 1995) and JASP (0.18.2.0, JASP Team, 2024) were used for analysis.

2.4. Stimulus properties

See Fig. 1 for a schematic illustration of a typical trial. All stimuli were presented on a black background (RGB: 0, 0, 0). A click on the central start box (1.93° × 1.93°) was required to initiate a trial. Upon trial initiation, a white fixation cross (0.78° × 0.78°) was presented at the screen center, and four gray (R = 169, G = 169, B = 169) response boxes (1.93° × 1.93°) at equidistant (8.66°) cardinal directions (left, right, up, down) from fixation. For the horizontal Simon task, a red (RGB: 255, 0, 0; CIE color coordinates: x = 0.581, y = 0.346) or green (RGB: 0, 255, 0; CIE color coordinates: x = 0.285, y = 0.599) circle (1.51° × 1.51°) was randomly presented to either the left or right side of the fixation cross. For the vertical Simon task, a yellow (RGB: 255, 255, 0; CIE color coordinates: x = 0.388, y = 0.513) or blue (RGB: 0, 0, 255; CIE color coordinates: x = 0.152, y = 0.080) circle appeared randomly above or below the fixation cross. The target circles were also presented at the same cardinal directions equidistant from the screen center but closer than the response boxes (5.99°).

2.5. Procedure

Participants were provided with informed consent and instructions on the experimental procedure. The experiment was carried out in a sound-proof chamber with dim lighting. Throughout the experiment, the midline of their bodies was aligned with the center of the monitor. The participants were required to click the start box to begin each trial within 1500 ms (see Fig. 1). Once the start box was clicked, the fixation cross and four response boxes appeared which lasted until the end of the trial, unless a response was registered. The target stimulus which followed 500 ms after, was presented briefly for 250 ms. Participants were instructed to move the mouse and click the response box indicated by the color of the target as fast and accurately as possible while ignoring the location of the target. If participants moved the mouse before the target was displayed, the mouse position was reset to the center of the display at the onset of the target. Responses that failed to initiate (leave the starting area) within 2000 ms were registered as incorrect. As soon as the response was complete, a blank intertrial display was presented for 1000 ms. Auditory feedback (750 Hz for 150 ms) was provided during this intertrial display for an incorrect response or a late response with a reaction time exceeding 2250 ms (Fig. 1).

The horizontal and vertical Simon tasks with non-overlapping stimuli and response sets were presented in an alternating trial-by-trial manner to prevent the repetition priming effects of stimulus and/or response features (Kim & Cho, 2014; Schmidt & Weissman, 2014). The pairings between the response box and target color were LEFT-RED, RIGHT-GREEN for the horizontal, and UP-YELLOW, DOWN-BLUE for the vertical Simon task. The target appeared randomly at left or right (horizontal) and up or down (vertical) locations. Note that the conflicting response buttons were diametrically opposite from each other rather than being at typical upper right or left corners frequently observed in mouse/hand tracking studies. The diametric layout increased the cost of movements in the wrong direction (Buetti & Kerzel, 2008; Wirth, Foerster, Kunde, & Pfister, 2020), which is methodologically advantageous for observing response conflicts. Except for the first and second trials of each block, stimuli were presented in a pseudo-random order to equate the number of trials for each congruency sequence type: congruent trials following a congruent trial (cC), congruent trials following an incongruent trial (iC), incongruent trials following a congruent trial (cI), and incongruent trials following an incongruent trial (iI). The congruency of the first two trials of each block was randomly assigned. A practice block of 30 trials was given followed by 6 main blocks each containing 82 trials. A 60-s break was provided between two blocks.

2.6. Analysis

2.6.1. Preprocessing

The mouse trajectory data were preprocessed before conducting statistical analyses. Bad trials were excluded first which included, outlier trials with RT faster or slower than 2.5 standard deviations of RT collapsed across all trial types (373 trials, 2.53 %), the trials immediately following the outlier trials (373 trials, 2.53 %), the first two trials of each block (360 trials, 2.44 %), the trials in which the cursor failed to leave the starting area within 2000 ms (4 trials, 0.03 %), incorrect trials (78 trials, 0.53 %), and the trials immediately following incorrect trials (77 trials, 0.52 %). As a result, a total of 1141 trials[1] were excluded from 14,760 trials collected from 30 participants, which comprised about 7.73 % (SD: 0.81 %, Range: 5.89–9.15 %) of the entire data. The remaining mouse trajectory data were resampled, using linear interpolation, to have 101 equally time-spaced points for each trial so that all trials contained the same number of data points, hence allowing for comparisons across trials and within-subject variables. All mouse trajectories were rotated and flipped towards the right such that all trajectories started at the center of the start box and ended at the right response box.

2.6.2. Discrete features

Grand averages of the preprocessed data were used to plot the mouse trajectory as in Fig. 2. A series of discrete and dynamic features were derived from the trajectory data for analysis. For discrete spatial

[1] Some of the trials fell within two or more exclusion criteria, which led to the exclusion of trials less than the sum of trials that fell within each criterion.

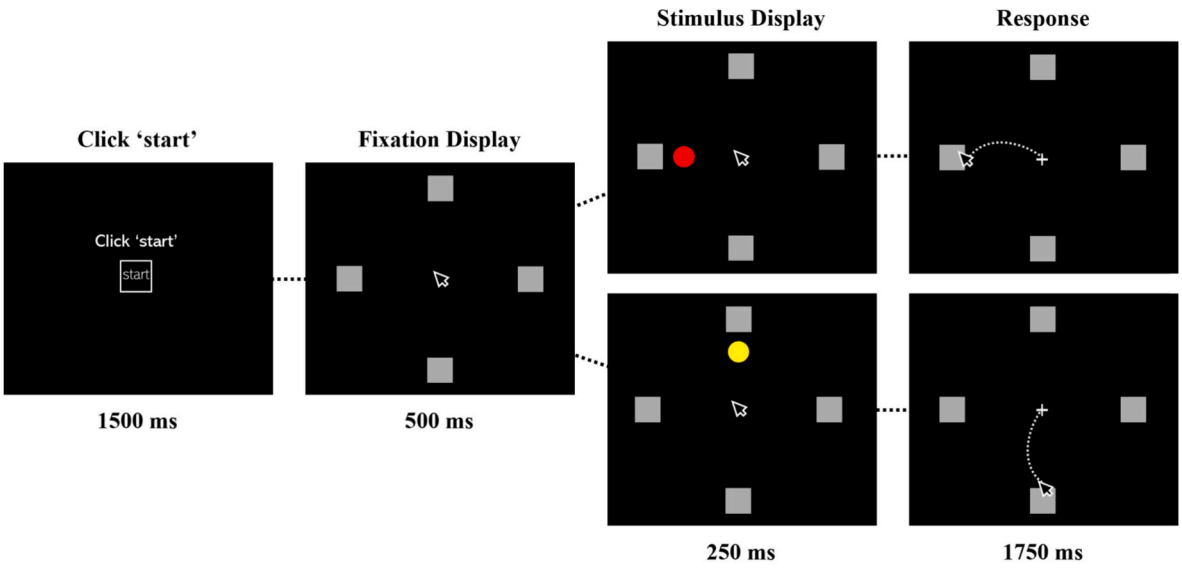

Fig. 1. Example illustration of the sequence of events in a trial. Vertical and horizontal Simon tasks alternated on a trial-by-trial basis. Each task had independent stimulus and response sets comprised of two alternative force choice responses. Participants were instructed to rapidly and accurately move the computer mouse cursor from the screen center to the correct response box upon presentation of the target stimulus. The target appeared in a location (task-irrelevant information) that was either congruent or incongruent with the location indicated by the stimulus color (task-relevant information).

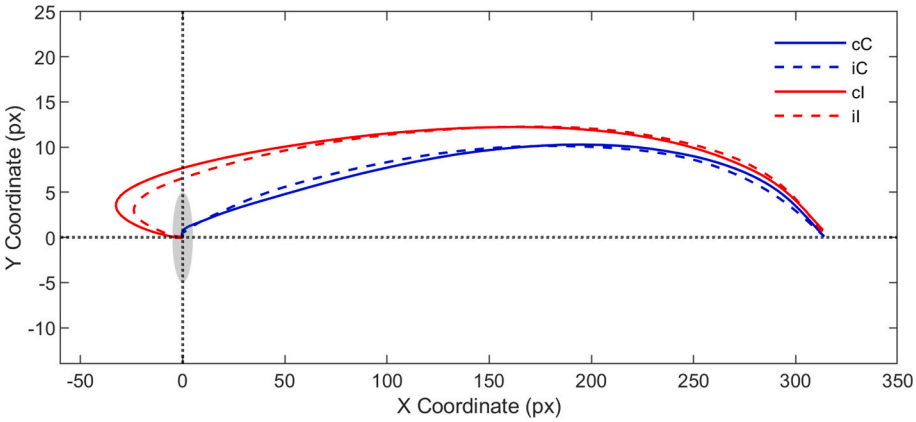

Fig. 2. Mouse trajectories from the starting coordinate (0-px, 0-px) to the center of the correct response location (0-px, 314-px) averaged by previous (N^{-1}) and current (N^0) trial congruency. The gray circle (vertically elongated) represents the cutoff threshold (5-pixel radius) for movement initiation dividing the initiation time (IT) and movement time (MT). On N^0 incongruent trials, the movement was pulled towards the task-irrelevant stimulus location (towards the left on the chart), showing a spatial Simon effect. The difference between the solid and dotted lines reflects the sequential modulations of cognitive control.

features, the minimum of the x-coordinates (X_{min}) and the trajectory length (T_{length}) were analyzed to estimate the amount of spatial deviation. X_{min} was defined by the furthest x-coordinate of the pixel from the target response box, which reflects spatial deviations towards the task-irrelevant location evident in N^0 incongruent trials. X_{min} is analogous to the maximum absolute deviation (MAD) of the curvature that typically measures deviations perpendicular to line connecting the starting point and the target destination (i.e., the y-axis). However, X_{min} reflects spatial deviation along the x-axis due to the diametric layout used in the current study. T_{length} was measured by the accumulated Euclidean distance in pixels between each time step.

The discrete latency features included the response time (RT) for completing the mouse click, the response initiation time (IT), and the movement time (MT). IT was defined as the time elapsed between the target onset and the mouse cursor leaving the movement threshold for the first time. A movement threshold of 5-px was used as a focal threshold near the starting point, aligning closely with the conventional threshold used for IT measurement for key-release responses (e.g., N. Lee & Cho, 2024). MT was the residual latency after subtracting IT from RT.

For all discrete measures (RT, IT, MT, X_{min}, T_{length}), two-way repeated measures ANOVA tests were performed for N^0 congruency (current trial) and N^{-1} congruency (previous trial). The main effect of N^0 tested for the standard Simon effect (N^0 incongruent – N^0 congruent) and the main effect of N^{-1} measured post-conflict slowing (N^{-1} incongruent – N^{-1} congruent). The interaction between N^{-1} and N^0 tested the CSE (N^{-1} incongruent Simon Effect – N^{-1} congruent Simon Effect). For all features that showed a significant CSE, further rm. ANOVAs were conducted to compare simple effects of previous congruency separately on N^0 congruent (iC – cC) and N^0 incongruent (iI - cI) trials. For each test, Bayes factors were calculated using JASP's Bayesian rm ANOVA (see Van den Bergh, Wagenmakers, & Aust, 2023, for the MRE method). We report the inclusion Bayes Factor (BF_{incl}) for significant results and the exclusion Bayes Factor (BF_{excl}) for non-significant results. Both BF_{incl} and BF_{excl} are interpreted in a similar way to conventional Bayes Factors and inverse Bayes Factors. BF_{incl} above 3 is considered at least moderate

evidence in favor of the alternative hypothesis over the null hypothesis. BF_{excl} above 3 indicates at least moderate evidence for the null hypothesis over the alternative hypothesis.

2.6.3. Dynamic features

Of greater concern in the current study was the temporal dynamics of the mouse movements. First, temporal dynamics in the x-coordinates ($X_{dynamic;}$ simply the x-coordinate of the mouse cursor plotted at each timestep) showed changes in spatial deviations from the current target location observed at each timestep. It can be expected that $X_{dynamic}$ coordinates in N^0 incongruent trials will be more negative across a wide range of timesteps than in N^0 congruent trials, since deviations occur in the direction opposite to the target location. Another crucial dynamic feature was movement speed, measured in pixels traveled per millisecond. Increases and decreases in speed also represented acceleration and deceleration. The speed at each time step was calculated by dividing the travel distance by the travel time between two neighboring time points, which resulted in 100-time steps, one less than the original 101 time points. Furthermore, the trajectory angle was analyzed to capture early direction changes in the movement even before the movement fully unfolded (Scherbaum et al., 2018). Trajectory angle changes were calculated by taking the inverse tangent of the distances traveled along the x and y axes, from one time-step to the next step, which also resulted in 100-time steps. Since all mouse trajectories were realigned rightward such that the trajectories were parallel to the x-axis, an angle of positive radians indicated a counterclockwise deviation from the ideal path to the target response box.

For all dynamic measures, the same tests as the discrete measures were performed, but multiple times on each time step. The acquired vector of *p*-values was adjusted for multiple comparisons (false discovery rate) and clusters of consecutively significant p-values shorter than 5-time steps were ignored. Summary statistics for the average of the significant clusters are provided together with the results of the multiple comparison data. For tests without significant clusters, all time steps were averaged into a single cluster to provide summarized statistics. Bayes factors for these clusters were computed in a way similar to those for discrete features.

3. Results

The grand averaged movement trajectory of the mouse cursor as a function of N^{-1} and N^0 trial congruency is shown in Fig. 2. Note that in Fig. 2, movement directions were rearranged so that the location of the response box is at the furthest right location at coordinate (0, 314) in pixels. In the current experimental design, response conflict occurred along the negative direction of the x-axis. As a result, movement in the N^0 incongruent trials appear *pointy* towards the left.

3.1. Discrete spatial features (X_{min} / T_{length})

Table 1 shows a summary of the descriptive statistics for all the discrete features. The minimum value of the x-coordinate (X_{min}), and trajectory length (T_{length}) were used to measure the amount of spatial deviation of the mouse movement towards the task-irrelevant location (i.e., the *spatial* Simon effect). Significant Simon effects (N^0 congruency) were observed in X_{min} and $T_{length.}$ On N^0 incongruent trials, X_{min} values were 41 pixels further from the target, $F(1, 29) = 38.126$, $p < .001$, $MSE = 51{,}936$, $\eta_p^2 = 0.568$, $BF_{incl} = 1.472 \times 10^8$, and T_{length} was 89 pixels longer than N^0 congruent trials, $F(1, 29) = 44.534$, $p < .001$, $MSE = 238{,}377$, $\eta_p^2 = 0.606$, $BF_{incl} = 4.678 \times 10^8$. Spatial precision was improved following N^{-1} incongruent trials; X_{min} coordinates were 5 pixels closer towards the target location, $F(1, 29) = 17.553$, $p < .001$, $MSE = 650$, $\eta_p^2 = 0.337$, $BF_{10} = 80{,}794$, and T_{length} was 11 pixels shorter than following N^{-1} congruent trials, $F(1, 29) = 17.997$, $p < .001$, $MSE = 3114$, $\eta_p^2 = 0.383$, $BF_{incl} = 74{,}585$.

The CSE ($N^{-1} \times N^0$ interaction) was also observed in X_{min}, $F(1, 29) = 25.234$, $p < .001$, $MSE = 1490$, $\eta_p^2 = 0.465$, $BF_{incl} = 105{,}715$, showing that a − 48-px Simon effect following N^{-1} congruent trials reduced to −35-px following incongruent trials. In $T_{length,}$ a 104-pixel Simon effect following N^{-1} congruent trials reduced to 76-px after incongruent trials, $F(1, 29) = 25.144$, $p < .001$, $MSE = 6363$, $\eta_p^2 = 0.464$, $BF_{incl} = 83{,}940$. Simple effect tests revealed that on N^0 congruent trials following N^{-1} incongruent trials (iC), compared to trials following N^{-1} congruent trials (cC), X_{min} was further away from the target location by 2 pixels, $F(1, 29) = 4.389$, $p = .045$, $MSE = 86$, $\eta_p^2 = 0.131$, $BF_{incl} = 1.398$, but T_{length} was not significantly longer, $F(1, 29) = 2.387$, $p = .133$, $MSE = 287$, $\eta_p^2 = 0.076$, $BF_{excl} = 1.453$. However, for N^0 incongruent trials after N^{-1} incongruent trials (iI) compared to N^{-1} congruent trials (cI), X_{min} was 11 pixels closer to the target location, $F(1, 29) = 26.837$, $p < .001$, $MSE = 2054$, $\eta_p^2 = 0.481$, $BF_{incl} = 918$, and T_{length} was significantly shorter by 25 pixels, $F(1, 29) = 30.048$, $p < .001$, $MSE = 9190$, $\eta_p^2 = 0.509$, $BF_{incl} = 1911$.

3.2. Discrete latency features (RT / IT / MT)

The typical Simon effect was replicated in RT findings showing that N^0 incongruent trials were delayed by 66 ms compared to N^0 congruent trials, $F(1, 29) = 73.553$, $p < .001$, $MSE = 129{,}786$, $\eta_p^2 = 0.717$, $BF_{incl} = 1.190 \times 10^9$. Post-conflict slowing did not occur in RT, $F(1, 29) = 1.710$, $p = .201$, $MSE = 242$, $\eta_p^2 = 0.056$, $BF_{excl} = 0.003$. There was a significant CSE, with the Simon effect reduced by 20 ms following N^{-1} incongruent trials compared to following N^{-1} congruent trials, $F(1, 29) = 19.624$, p

Table 1
Summary of statistics for discrete latency and spatial measures.

DV	cC	cI	iC	iI	Simon Effect	Post-Conflict Slowing	CSE	iC – cC	iI – cI
	M (SD) (CI_{lower} – CI_{upper})								
RT (ms)	758 (63) (736–781)	834 (61) (813–856)	771 (66) (748–795)	827 (70) (802–852)	66***	3	−20***	13***	−7*
IT (ms)	351 (76) (324–379)	368 (81) (339–397)	364 (77) (337–391)	379 (85) (348–409)	16***	12***	−2	13***	11***
MT (ms)	407 (51) (389–425)	466 (86) (435–497)	407 (53) (389–426)	449 (92) (416–481)	51***	−9**	−17**	0	−17***
X_{min} (px)	−6 (7) (−8 - −3)	−54 (46) (−71 - −38)	−8 (12) (−12 - −4)	−43 (42) (−58 - −28)	−42***	5***	13***	−2*	11***
Tlength (px)	348 (30) (337–359)	452 (107) (413–490)	352 (39) (338–366)	427 (97) (392–462)	90***	−11***	−29***	4	−25***

Notes: The movement threshold for IT is 5 pixels. X_{min} is the maximum deviation towards the opposite direction from starting point to the target location. For cC, cI, iC, and iI, the lower case represents N^{-1} congruency, and the upper case represents N^0 congruency, while 'c' stands for congruent and 'i' for incongruent. Equations for the Simon Effect (N^0 incongruent – N^0 congruent); the post-conflict slowing (N^{-1} Incongruent – N^{-1} congruent), and the CSE (N^{-1} Incongruent Simon Effect – N^{-1} Congruent Simon Effect). * = (p < .05), ** = (p < .01), *** = (p < .001). The underlined values indicate that the direction of the BF_{incl} or BF_{excl} was in agreement with the NHST tests.

$< .001$, $MSE = 3027$, $\eta_p^2 = 0.404$, $BF_{incl} = 1577$. Simple comparisons revealed that RT was significantly delayed after iC trials by 13 ms compared to cC trials, $F(1, 29) = 20.579$, $p < .001$, $MSE = 2489$, $\eta_p^2 = 0.415$, $BF_{incl} = 202$. RT was significantly facilitated by 7 ms on iI compared to cI trials, $F(1, 29) = 4.464$, $p = .043$, $MSE = 779$, $\eta_p^2 = 0.133$, $BF_{10} = 1.49$. RT results were consistent with previous observations indicating that post-conflict slowing is diluted by the CSE in RT measures (Verguts et al., 2011).

Response time was divided into two discrete latencies representing the earlier response initiation time (IT) and the later movement time (MT) using a movement threshold of 5 pixels in radius (see analysis section). IT demonstrated a significant 51-ms Simon effect, $F(1, 29) = 52.036$, $p < .001$, $MSE = 7480$, $\eta_p^2 = 0.415$, $BF_{incl} = 215{,}714$. The main effect of N^{-1} congruency was significant in IT, $F(1, 29) = 59.710$, $p < .001$, $MSE = 3875$, $\eta_p^2 = 0.673$, $BF_{incl} = 58{,}137$, indicating post-conflict slowing of 12-ms. No CSE was observed in IT, $F(1, 29) < 1$, $BF_{excl} = 0.80$. More specifically, iI trials were 11 ms faster than cI trials, $F(1, 29) = 22.452$, $p < .001$, $MSE = 1574$, $\eta_p^2 = 0.436$, $BF_{10} = 330$. Also, iC trials were significantly slower than cC trials by 13 ms, $F(1, 29) = 28.082$, $p < .001$, $MSE = 2338$, $\eta_p^2 = 0.492$, $BF_{incl} = 1228$. The lack of evidence for the CSE in IT indicates that post-conflict slowing and the CSE occur in distinct temporal stages.

Meanwhile, the Simon effect was observed in MT, showing that the mean latency was 51 ms slower on incongruent trials ($M = 458$ ms) than on congruent trials ($M = 407$ ms), indicated by a significant main effect of N^0 congruency, $F(1, 29) = 37.226$, $p < .001$, $MSE = 74{,}952$, $\eta_p^2 = 0.562$, $BF_{incl} = 283{,}393$. Post-conflict *facilitation* was observed in MT, $F(1, 29) = 9.966$, $p = .004$, $MSE = 2182$, $\eta_p^2 = 0.256$, $BF_{incl} = 112$, showing that responses were 9 ms faster following an N^{-1} incongruent trial ($M = 428$ ms) than following an N^{-1} congruent trial ($M = 437$ ms).

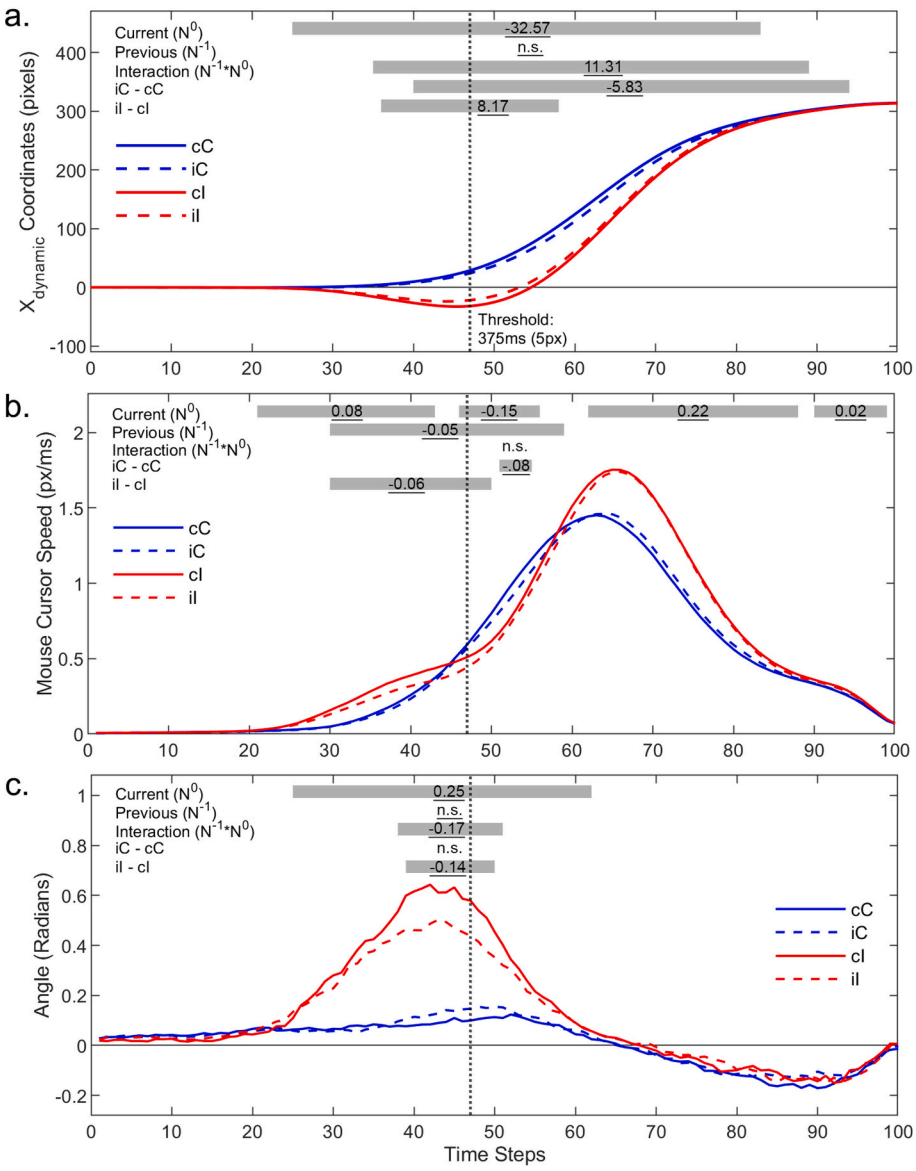

Fig. 3. Charts showing dynamics of the mouse movement measured in $X_{dynamic}$ coordinates (pixels), movement speed (pixels/ms), and trajectory angle change (radians) by previous (N^{-1}) and current (N^0) trial congruency. The 0th and 100th time step respectively indicates the beginning of the trial and the latency of movement termination. The upper gray bars indicate the time ranges of significant clusters from mass univariate ANOVAs corrected for multiple comparisons. The values in the gray bars indicate the average value of the clusters of corresponding statistical tests. The vertical dotted lines represent the mean IT determined by the movement threshold of 5-pixels (radius). (a) $X_{dynamic}$ coordinates (y-axis) in which smaller y-values in the graph indicate greater spatial deviation. (b) Speed dynamics in which greater y values indicate greater speed. A positive slope indicates acceleration while a negative slope indicates deceleration. (c) Angle dynamics in which higher radian values indicate a counterclockwise angle deviation from the straight path towards the target. The underlined values indicate that the direction of the BF_{incl} or BF_{excl} values from the averaged clusters was in agreement with the NHST tests.

There was a significant CSE in MT, $F(1, 29) = 11.883$, $p = .002$, $MSE = 2389$, $\eta_p^2 = 0.291$, $BF_{incl} = 157$, showing that a 59 ms Simon effect following N^{-1} congruent trials was reduced to 42 ms following N^{-1} incongruent trials. Simple effect analysis revealed that MT was significantly faster by 17 ms on iI trials than cI trials, $F(1, 29) = 17.639$, $p < .001$, $MSE = 4569$, $\eta_p^2 = 0.378$, $BF_{incl} = 92$. However, iC trials were not significantly different than cC, $F(1, 29) < 1$, $BF_{excl} = 3.362$ showing moderate evidence in favor of null.

3.3. Continuous dynamics (Xdynamic, Speed, Angle)

$X_{dynamic}$ coordinates. Fig. 3a shows the temporal dynamics of the mouse cursor position along the path towards the response box (the straight path from start to finish along the x-axis in Fig. 2). X_coordinates of Fig. 2 are plotted as the y-axis in Fig. 3a and time steps are plotted on the x-axis of Fig. 3a. The average latency of the 100th time step was 798 ms. The analysis revealed distinct spatial profiles between N^0 congruent and N^0 incongruent trials. Results show that the mouse movement significantly lagged on N^0 incongruent trials compared to N^0 congruent trials as shown by a single cluster between the 25th and 83rd time steps (199–662 ms, all corrected $ps < 0.05$) by 33 pixels on average, $F(1, 29) = 70.681$, $p < .001$, $MSE = 225$, $\eta_p^2 = 0.709$, $BF_{incl} = 3.666 \times 10^8$. There was no significant cluster modulated by N^{-1} congruency, and no overall effect was observed across all time steps (all corrected $ps > 0.05$), $F(1, 29) < 1$, $BF_{excl} = 3.307$.

The CSE was present in a single cluster between the 35th and 89th time steps (279–710 ms, all corrected $ps < 0.05$), $F(1, 29) = 30.713$, $p < .001$, $MSE = 31$, $\eta_p^2 = 0.514$, $BF_{incl} = 270{,}761$. Further analyses revealed that x-coordinates on iC trials lagged behind cC trials in a single cluster between the 40th and 94th time steps (319–750 ms, all corrected $ps < 0.05$) by 5.833 pixels on average, $F(1, 29) = 32.659$, $p < .001$, $MSE = 16$, $\eta_p^2 = 0.530$, $BF_{incl} = 3313$. The $X_{dynamic}$ coordinates on iI trials surpassed the coordinates of cI trials between the 36th and 58th time steps (287–463 ms) by 8.173 pixels on average, $F(1, 29) = 18.943$, $p < .001$, $MSE = 54$, $\eta_p^2 = 0.395$, $BF_{incl} = 129$.

Movement Speed. Fig. 3b shows the temporal dynamics of the mouse cursor movement speed in each timestep. The analysis revealed distinct speed profiles between N^0 congruent and N^0 incongruent trials. Speed dynamics of N^0 congruent trajectories (blue lines) were simple, showing a single acceleration-deceleration pattern. In contrast, the speed dynamics of incongruent trajectories (red lines) were more complex, with an additional small fluctuation in acceleration that can be visually identified before the 60th time step (before 472 ms).

There were four significant clusters of N^0 congruency main effects. Two clusters occurred earlier than the 60th time step. The first cluster was observed between 21st and 42nd time steps (168–335 ms, all corrected $ps < 0.05$), with a mean speed difference of 0.083 pixels/ms showing *faster* incongruent trials faster by a mean speed of 0.083 pixels/ms, $F(1, 29) = 20.457$, $p < .001$, $MSE = 0.005$, $\eta_p^2 = 0.414$, $BF_{incl} = 194$. The second cluster showed significantly slower incongruent trials with a mean speed difference of −0.154 pixels/ms observed between 46th and 55th time steps (367–439 ms, all corrected $ps < 0.05$), $F(1, 29) = 30.659$, $p < .001$, $MSE = 0.012$, $\eta_p^2 = 0.514$, $BF_{incl} = 2184$. The third cluster was observed between the 62nd and 87th time steps (495–694 ms, all corrected $ps < 0.05$) with a significant mean speed difference of 0.22-px/ms also showing strong evidence towards the alternative, $F(1, 29) = 129$, $p < .001$, $MSE = 0.006$, $\eta_p^2 = 0.816$, $BF_{incl} = 1.475 \times 10^9$. The fourth significant cluster was observed between the 90th and 99th time steps (718–490 ms, all corrected $ps < 0.05$) with an average of 0.019 pixels/ms, $F(1, 29) = 14.393$, $p < .001$, $MSE = 0.0004$, $\eta_p^2 = 0.332$, $BF_{incl} = 37$.

Trajectory speed also revealed post-conflict slowing; Trajectory speed was slower following N^{-1} incongruent ($M = 0.52$ pixel/ms) trials than N^{-1} congruent ($M = 0.57$-px/ms) trials between 30th and 59th time steps (239–471 ms, all corrected $ps < 0.05$) with an average speed difference of −0.045 pixel/ms, $F(1, 29) = 46.499$, $p < .001$, $MSE = 0.0006$, $\eta_p^2 = 0.616$, $BF_{incl} = 46{,}458$. The CSE did not reach significance in movement speed at any given time steps (all corrected $ps > 0.05$). However, there was a significant CSE when all time steps were averaged as a single cluster, $F(1, 29) = 18.629$, $p < .001$, $MSE = 0.0002$, $\eta_p^2 = 0.391$, $BF_{incl} = 5401$. This may indicate that an interaction is distributed across the time steps but overall does not significantly affect a specific timepoint. Movement speed was significantly slower by 0.08 pixels/ms on iC than cC trials between the 51st and 55th time steps (407–439 ms), $F(1, 29) = 14.261$, $p < .001$, $MSE = 0.006$, $\eta_p^2 = 0.330$, $BF_{incl} = 35$. Speed was also significantly slower on iI than cI trials by 0.059 pixels/ms between the 30th and 50th time steps (239–399 ms), $F(1, 29) = 27.508$, $p < .001$, $MSE = 0.002$, $\eta_p^2 = 0.487$, $BF_{incl} = 1086$.

Trajectory Angle. The trajectory angle change between adjacent time points at each time step is shown in Fig. 3c. Movement direction from the center of the starting location towards the center of the target response box is represented as 0 rad. If mouse movements deviate counterclockwise from this shortest course of movement, angular changes should occur in positive radian values. The angle dynamics result shows that the movement direction on congruent trials was closely aligned with 0 rad. In comparison, the trajectory angles of the incongruent trials show greater deviance in the counterclockwise direction reflective of the response conflict.

A direct comparison at each time step revealed one significant cluster of the Simon effect in trajectory angles between the 25th and 62nd time steps (199–495 ms, all corrected $ps < 0.05$) with an average difference of 0.246 rad, $F(1, 29) = 70.156$, $p < .001$, $MSE = 0.013$, $\eta_p^2 = 0.708$, $BF_{incl} = 2.166 \times 10^7$. There was no significant N^{-1} congruency effect at all time points (all corrected $ps > 0.05$) and the average of the all time steps was also not significant $F(1, 29) = 2.004$, $p = .168$, $MSE = 0.0002$, $\eta_p^2 = 0.065$, $BF_{excl} = 1.267$. A single cluster was observed for the CSE between the 38th and 51st time steps (304–408 ms, all corrected $ps < 0.05$). The Simon effect on N^{-1} congruent trials of 0.47 rad reduced to 0.3 rad on N^{-1} incongruent trials, $F(1, 29) = 55.036$, $p < .001$, $MSE = 0.004$, $\eta_p^2 = 0.655$, $BF_{incl} = 5.691 \times 10^7$. Further analysis revealed that angle deviations on iI trials reduced by an average of 0.137 rad compared to cI trials, between 39th and 50th time steps (311–399 ms, all corrected $ps < 0.05$), $F(1, 29) = 40.468$, $p < .001$, $MSE = 0.007$, $\eta_p^2 = 0.583$, $BF_{incl} = 15{,}350$. Angle deviations on iC trials were not significantly different from cC trials (all corrected $ps > 0.05$). When considering all time steps as a single cluster, the angle deviated further by 0.009 rad on iC trials compared to cC trials, $F(1, 29) = 5.970$, $p = .021$, $MSE = 0.0002$, $\eta_p^2 = 0.171$, $BF_{incl} = 2581$. This likely indicates that a small control effect was distributed across the all time steps between iC and cC trials, resulting in only weak angle deviations when averaging across the entire time range.

3.4. Repetition priming from N^{-2} is minimized

Feature/response repetition between N^0 and N^{-2} can have a lingering influence on performance, even in the confound minimized cross-task design (Erb & Aschenbrenner, 2019). The most direct way of testing whether feature repetitions from N^{-2} have an impact on N^0 trials is to look at the main effect of N^{-2} feature repetition. Responses are generally facilitated after feature repetitions, but we observed no evidence of such facilitation. No main effect of repetition priming was observed in all discrete measures (all $ps < 0.05$) which indicates that there is a minimal influence from feature repetitions.

Furthermore, a control analysis was conducted on the Simon effect (N^0 congruency) by a function of N^{-1} congruency and congruency repetition between N^{-2} and N^{-1} as done in Lim and Cho (2021a). This analysis can test for repetition priming, as cognitive control and repetition priming produce similar patterns of CSE following congruency repetition but opposite patterns following congruency switches, which diminishes the CSE. Combining the repetition and switch trials averages out the impact of N^{-2} repetition priming but the impact of control is unaffected which shows that cross-task designs minimize repetition confounds. Another advantage is that the test can assess the effect based on top-down expectations of congruency repetitions (see discussion).

Consistent with the null main effect of feature repetitions, the follow-up control analysis also shows signs of minimized repetition confounds from N^{-2} trials.

RM ANOVA revealed significant interactions of N^{-2} congruency repetition and N^{-1} congruency type on the Simon effect for RT, $F(1, 29) = 36.140$, $p < .001$, $MSE = 994$, $\eta_p^2 = 0.555$, $BF_{incl} = 1.098 \times 10^8$, IT, $F(1, 29) = 15.871$, $p < .001$, $MSE = 219$, $\eta_p^2 = 0.354$, $BF_{incl} = 104$, MT, $F(1, 29) = 17.024$, $p < .001$, $MSE = 1001$, $\eta_p^2 = 0.370$, $BF_{incl} = 7012$, T_{length}, $F(1, 29) = 21.449$, $p < .001$, $MSE = 1235$, $\eta_p^2 = 0.425$, $BF_{incl} = 206{,}388$, X_{min}, $F(1, 29) = 29.073$, $p < .001$, $MSE = 165$, $\eta_p^2 = 0.501$, $BF_{incl} = 363{,}960$, and dynamic features of $X_{dynamic}$, [a cluster between 30th and 72nd time steps (239–574 ms), $F(1, 29) = 35.111$, $p < .001$, MSE = 112, $\eta_p^2 = 0.548$, $BF_{incl} = 2.433 \times 10^6$]. No significant clusters were observed for angle and speed (all $ps > 0.05$).

Significant CSEs were observed after repetitions in RT, $F(1, 29) = 34.798$, $p < .001$, $MSE = 1313$, $\eta_p^2 = 0.545$, $BF_{incl} = 18{,}899$, IT, $F(1, 29) = 10.688$, $p < .001$, $MSE = 296$, $\eta_p^2 = 0.269$, $BF_{incl} = 22$, MT, $F(1, 29) = 21.369$, $p < .001$, $MSE = 1161$, $\eta_p^2 = 0.424$, $BF_{incl} = 329$, T_{length}, $F(1, 29) = 25.433$, $p < .001$, $MSE = 1960$, $\eta_p^2 = 0.467$, $BF_{incl} = 746$, X_{min}[$F(1, 29) = 31.86$, $p < .001$, $MSE = 322$, $\eta_p^2 = 0.523$, $BF_{incl} = 2795$, $X_{dynamic}$, [a cluster between 33rd and 97th time steps (263–774 ms), $F(1, 29) = 43.888$, $p < .001$, $MSE = 115$, $\eta_p^2 = 0.602$, $BF_{incl} = 32{,}194$], Angle [a cluster between 37th and 51st time steps (295–407 ms), $F(1, 29) = 38.478$, $p < .001$, $MSE = 0.0255$, $\eta_p^2 = 0.570$, $BF_{incl} = 15{,}093$], and Speed [a cluster between 30th and 36th time steps (239-287 ms), $F(1, 29) = 14.146$, $p < .001$, $MSE = 0.00459$, $\eta_p^2 = 0.328$, $BF_{incl} = 34$].

CSEs were not significant after alternations in IT, $F(1, 29) = 2.691$, $p = .112$, $MSE = 275$, $\eta_p^2 = 0.085$, $BF_{incl} = 0.916$, MT, $F(1, 29) = 1.133$, $p = .296$, $MSE = 646$, $\eta_p^2 = 0.038$, $BF_{incl} = 0.426$, T_{length}, $F(1, 29) < 1$, $MSE = 240$, $\eta_p^2 = 0.007$, $BF_{incl} = 0.281$, and X_{min}, $F(1, 29) < 1$, $MSE = 72$, $\eta_p^2 = 0.006$, $BF_{incl} = 0.283$. No clusters were observed for all dynamic measures (all $ps > 0.05$). However, a reversed CSE was observed in RT after alternations, $F(1, 29) = 8.866$, $p = .006$, $MSE = 332$, $\eta_p^2 = 0.234$, $BF_{incl} = 6.798$.

Further tests were conducted testing whether feature repetitions from N^{-2} trials had a lingering effect on the cross task CSE by testing for a significant interaction between N^{-1} congruency and feature repetition between N^{-1} and N^{-2} trials. There were no significant interactions in RT, $F(1, 29) < 1$, $MSE = 696$, $\eta_p^2 = 0.015$, $BF_{incl} = 0.916$, IT, $F(1, 29) = 1.857$, $p = .183$, $MSE = 266$, $\eta_p^2 = 0.060$, $BF_{incl} = 0.916$, and MT, $F(1, 29) = 3.732$, $p = .063$, $MSE = 428$, $\eta_p^2 = 0.114$, $BF_{incl} = 0.916$, but there were significant interactions in T_{length}, $F(1, 29) = 9.564$, $p = .004$, $MSE = 597$, $\eta_p^2 = 0.248$, $BF_{incl} = 0.916$ and X_{min}, $F(1, 29) = 11.49$, $p = .002$, $MSE = 100$, $\eta_p^2 = 0.284$, $BF_{incl} = 0.916$.

4. Discussion

The present study used a confound-minimized cross-task design and computer mouse movements to test whether the sequential modulation of conflict in the Simon task stems from a unitary selective control mechanism, or from a combination of selective and domain-general control. Horizontal and vertical Simon tasks, each with independent stimulus and response sets, were presented in a trial-by-trial alternating order to avoid repetition priming and contingency learning. Error and post-error trials were removed to focus on the impact of pure response conflicts. Previous studies using confound-minimized Simon task studies with key-release latency measures (e.g., Lim & Cho, 2021b), and a moderately controlled Simon task study using hand reaching (Erb & Marcovitch, 2019), have independently provided evidence of post-conflict slowing in early response latencies, and the CSE in the movement curvature and late response latencies. The current study provides both rigorous control over repetition priming and continuous measures of behavior that allow an overarching insight by bridging the previous findings. The current study further expands on the previous curvature results by performing a deeper analysis of the spatiotemporal dynamics (angle and speed) of the movement. Temporal dynamics allowed better estimation of the onset latency of post-conflict slowing and the CSE. Overall, the current results provide strong evidence supporting the dual-mechanism view of the sequential modulation activated by cognitive control.

4.1. Spatiotemporal dynamics of post-conflict slowing and the CSE

The basic N^0 congruency effect (the Simon Effect) was observed in the movement trajectory showing deviations towards the task-irrelevant location, consistent with limb movement literature on conflict tasks (Buetti & Kerzel, 2009; Erb et al., 2016; Erb & Marcovitch, 2019; Scherbaum et al., 2010, 2018; Welsh & Elliott, 2004; see Table 1 and Fig. 3). Angle dynamics further revealed that spatial deviation occurred early, although the Simon effect persisted in the overall movement until the termination of the response ($X_{dynamic}$). The early onset of the Simon effect is consistent with the dual-route models (De Jong, Liang, & Lauber, 1994; Ridderinkhof, 2002) that assume an automatic triggering of task-irrelevant response activations and its gradual suppression (Buetti & Kerzel, 2009; Ridderinkhof, 2002; Welsh & Elliott, 2004) or decay (Hommel, 1994).

Most importantly, the current study provides evidence of post-conflict slowing occurring concurrently with the CSE, which suggests post-conflict slowing operates independently during sequential control of response conflicts (Erb et al., 2019; Erb et al., 2021; Verguts et al., 2011). Our results show that post-conflict slowing affected distinguishable movement features and temporal latencies from the CSE. First, previous conflict types modulated movement speed in early latencies (See Fig. 3b) and IT (Table 1) without interacting with current conflict types, which shows characteristics of domain-general processing (i.e. post-conflict slowing). No sign of the CSE was evident in speed and IT. Rather, the CSE was evident in MT and all spatial measurements. Most notably, movement angle was selectively modulated by previous congruency when conflict was present on the current trial. This effectively reduced the distance for the mouse cursor to travel resulting in a decrease in overall latency, while the movement speed remained unbothered. This also implies that selective control operates through resolution of spatial conflict while the domain-general control has control over movement speed.

Furthermore, the onset latency of post-conflict slowing in speed (239 ms) was also faster than the onset of the CSE in angle (306 ms), which parallels the slowing effect in IT and the CSE in MT. The earlier onset of the slowing effect is consistent with the view that response criterion shifts occur rapidly (Wessel, 2018), before the next trial begins in the current design. In contrast, it is evident that the CSE, largely driven by selective control in iI vs. cI trials, occurs later only in response to the current target stimulus. There was also a considerable temporal overlap between the slowing effect and the CSE, suggesting that these effects are not neatly separated into discrete temporal stages of IT and MT. Rather, these two control processes are likely to arise from independent and parallel neural circuitry.

4.2. Post-conflict slowing is present during the CSE

Current results are consistent with a growing body of literature that identifies post-conflict slowing as an independent source of sequential modulation. A series of studies using confound-minimized Simon tasks with key-releases have shown post-conflict slowing in IT and the CSE in MT (Y. S. Lee & Cho, 2023; N. Lee & Cho, 2024; Lim & Cho, 2021b). A Simon task study using hand movement has also reported post-conflict slowing in IT, and the CSE in MT, hand movement curvatures, and change of mind in trials without feature repetition (Erb & Marcovitch, 2019). Although this study did not use a confound-minimized procedure, the MT and curvature results are consistent with the MT and $X_{dynamic}$ results of the current study. Nevertheless, there is substantial evidence that post-conflict slowing is a recurring phenomenon reliably observed during the CSE.

Erb and Marcovitch (2019) also reported performance costs in iC vs. cC trials in the change of mind measurement consistent with the $X_{dynamic}$ results of the current study and numerous previous studies (N. Lee & Cho, 2024; Y. S. Lee & Cho, 2023; Lim & Cho, 2021b; Verguts et al., 2011). The cause of the performance cost in the iC vs. cC trials was previously attributed to a unitary suppression mechanism. However, the performance cost is easily explained through post-conflict slowing. Verguts et al. (2011) demonstrated that the typical pattern of the CSE comprises of two components, by presenting congruent, neutral, or incongruent Simon primes, then measuring responses to a univalent probe containing just the task relevant dimension (color) or just the task-irrelevant dimension (location). Univalent probes do not contain response conflicts thus do not trigger selective control. Under such conditions, response conflicts in the prime always delayed responses. This was proof that the performance cost on iC vs. cC trials can be explained by post-conflict slowing.

Post-conflict slowing is incompatible with the unitary conflict adaptation account because conflict adaptation assumes that selective control is *pre-configured* following a previous conflict and does not depend on experiencing conflict on the current trial (Ridderinkoff, 2002; Scherbaum et al., 2010, 2018). Control can be selectively implemented via *suppression* of irrelevant response activations (Hübner & Mishra, 2013; Kim et al., 2015; J. Lee & Cho, 2013; Lee & Sewell, 2024; Ridderinkhof, 2002; Soutschek et al., 2013,Stürmer et al., 2002; Stürmer & Leuthold, 2003) or *amplification of* task-relevant stimulus features (Egner & Hirsch, 2005, Scherbaum et al., 2010, 2018, Verguts et al., 2011). The suppression view explained that performance costs can occur in iC vs. cC trials, because congruent task-irrelevant response activations no longer facilitate responses when suppressed (Ridderinkhof, 2002). The amplification view in contrast predicted improvements or no changes in performance. In any case, the prevailing evidence of post-conflict slowing in the literature is a compelling reason to re-consider how selective control operates.

4.3. Selective control is triggered by current conflict

Alternative to the view that selective control is pre-configured, evidence for selective control triggered by previous and current response conflicts is provided by previous EEG (Stürmer et al., 2002; Stürmer & Leuthold, 2003) and fMRI (Egner & Hirsch, 2005) studies. Stürmer et al. (2002) examined the sequential modulation of control by observing lateralized readiness potentials (LRPs) while participants made go-no-go responses to targets in a Simon task (Experiment 3). LRPs, which occur just before a response is initiated over the contralateral central scalp region near the motor-related cortices, serve as a marker of the summed response activations leading to an overt response. The authors observed that LRP activations on current incongruent trials were still affected by the task-irrelevant location, in spite of being suppressed when preceded by congruent trials. However, when preceded by an incongruent trial, LRPs on the current incongruent trials were not affected by stimulus location, indicating enhanced suppression. Meanwhile, LRPs on current congruent trials remained unaffected, which shows suppression is not triggered without the presence of another response conflict (also see Stürmer & Leuthold, 2003).

As further evidence of suppression, a recent EEG study employed a cross-task Simon task with key-release measurements and measured suppression effects in discrete frequency bands (Y. S. Lee, Bae, & Cho, 2025). This study found that decoding accuracy of the task-irrelevant location in the high beta frequency (20-30 Hz) was significantly above chance approximately between 400 and 500 ms when the previous trial was congruent. However, decoding accuracy significantly dropped when the previous trial was incongruent. Beta frequency is closely linked to modulation of responses which implies that automatic response activation to the task-irrelevant location in the subsequent trial can be suppressed after response conflicts.

Egner and Hirsch (2005) provide evidence for selective amplification in response to current response conflicts. Using a facial Stroop task with superimposed name distractors, authors showed that BOLD activation in the fusiform face area, increases after incongruent trials but only when the current trial was incongruent (see Fig. 2d in Egner & Hirsch, 2005). The activation was not observed when the names were targets and faces were distractors showing that the activity in the FFA is enhanced only when faces were task relevant (see Fig. 2e in Egner & Hirsch, 2005). Together, evidence presents that the sequential modulation of selective control occurs through detection of conflict in the following trial.

4.4. Is selective control suppression or amplification?

The remaining issue is whether selective control of the CSE reflects suppression or amplification after accounting for post-conflict slowing. The current study does not directly address this issue, and previous research has shown mixed findings. A possible solution to the problem is by assuming that cognitive control is highly flexible and different selective control modes can be selected based on the nature of the conflict provided by the primary task (Egner, 2008, 2014). In other words, amplification and suppression may be optimal mechanisms of control for managing different types of response conflict (see Braem et al., 2014 and Egner, 2008 for reviews).

One of the factors that determines whether suppression or amplification occurs is whether the task involves automatic spatial mappings between stimulus and response (S-R mapping). Suppression is the likely mechanism for Simon tasks, since strong response conflicts occur from stimulus-response compatibility. Consistent with this view, using stronger spatial features as task-irrelevant information (physical location > arrow > location-word) in the cross-task design led to stronger Simon effects and CSEs (N. Lee & Cho, 2024). Spatial representations of task-irrelevant stimulus location automatically activate responses (Proctor & Cho, 2006; Stürmer et al., 2002) and responses activate spatial representation also in reverse (Hommel, Müsseler, Aschersleben, & Prinz, 2001). Because the conflict between responses is so strong, an optimum strategy for the Simon task would be to suppress the erroneous response. Meanwhile, amplification of the task-relevant stimulus feature is a plausible strategy for the typical color-word Stroop task (with manual responses) or the letter flanker task (but not arrow flankers) because response to the task-irrelevant feature is not triggered automatically. In such cases, simply enhancing the processing of the task-relevant feature may suffice. In support of the importance of conflict types, Y. S. Lee et al. (2025) and Stürmer et al., 2002,Stürmer & Leuthold, 2003) provide EEG evidence of suppression using Simon tasks, while Egner and Hirsch (2005) provide evidence supporting amplification using a facial Stroop task and fMRI. A similar principle can be applied to flanker tasks without S-R conflicts (Hübner & Töbel, 2019; also see Luo & Proctor, 2022 for modelling results).

Given that response conflict magnitude varies according to the strength of the S-R mapping, the magnitude of the CSEs may have a smaller effect size in tasks with arbitrary S-R mappings as in typical color-word Stroop or letter flanker tasks. Smaller effect-size may sometimes lead to inconsistent observations of the CSE in these tasks. Indeed, CSEs have been consistently observed in the MT and curvatures in the current and previous confound minimized cross-task Simon tasks (N. Lee & Cho, 2024; Y. S. Lee & Cho, 2023; Lim & Cho, 2021b) as well as other moderately controlled Simon task studies (Erb & Marcovitch, 2019). Meanwhile, a significant CSE was observed in a three-response Stroop task that minimizes S-R bindings but not contingency learning (Erb et al., 2016: Exp 1), but the CSE disappeared once a stronger control method was used (Erb et al., 2019). In similar vein, the CSE was not observed in a less spatially effective letter flanker task (Erb et al., 2016: Exp 2) but was observed in a more spatially effective arrow flanker tasks (Lim & Cho, 2021b; Exp 3; Erb & Marcovitch, 2018) or letters flanker tasks with some spatial organization (alphabetical order) (Lim & Cho, 2018).

Furthermore, cross-task designs that intermix different conflict tasks

provide evidence that the strength of spatial conflict between S-R mapping can determine suppression or amplification during selective control. S-R mapping. Selective control is domain-specific and should not display sequential control when the source of conflict in following trials do not match the previous. Thus, CSEs (from selective control) are expected when alternating trials both use the same suppression or amplification mechanism for sequential control but not when these trials recruit different circuitry. Using this principle, studies have shown that Simon tasks do not generate CSEs in the following Stroop trial and the same is true in reverse (see Braem et al., 2014 and Egner, 2008 for reviews). CSEs even do not generalize between two different types of spatial conflicts: between Simon trials with actual task-irrelevant locations (strong S-R mapping) and Simon trials with task-irrelevant word representing the locations (weak S-R mapping; N. Lee & Cho, 2024). In sum, we speculate that how S-R mapping is configured in a given task determines whether selective control over repeating conflicts uses suppression or facilitation for optimal control.

4.5. Response facilitation after post-conflict slowing

Aside from selective control, other mechanisms could also influence the facilitatory effects observed in iI vs. cI trials in MT. For example, models predict a facilitation of response following speed-accuracy trade-offs alone (Miller & Schwarz, 2021). Delaying the execution of a response results in faster response onset because there was more time for suppressing the task-irrelevant response activations and also more time for the task-relevant response activation to build up (Miller & Schwarz, 2021). Facilitations can also strengthen under time pressure which occurs frequently in Simon tasks or other tasks with automatic S-R mappings (Mittelstädt, Miller, Leuthold, Mackenzie, & Ulrich, 2022). In the present study, MT showed a reverse post-conflict facilitation (an N^{-1} congruency effect) in addition to the CSE, which is presumably the result of the conservative criterion shifts in combination with a race to meet the deadline (e.g., Miller & Schwarz, 2021; Mittelstädt et al., 2022). However, EEG and fMRI studies have provided solid evidence for selective control (Egner & Hirsch, 2005; Y. S. Lee et al., 2025; Stürmer et al., 2002; Stürmer & Leuthold, 2003; also see Finkbeiner & Heathcote, 2016). Thus, it is likely that speed-accuracy trade-off accounts for only a small portion of the facilitation in iI trials. Future studies should address the extent to which post-conflict slowing contributes to the facilitatory behavioral effects in the CSE.

4.6. Post-conflict slowing trades speed for accuracy

The facilitation in iI vs. cI trials is due to selective control but what is the mechanism behind post-conflict slowing? Examining error-related studies, post-error slowing reflects a conservative shift in the response criteria trading speed for higher response accuracy (Botvinick et al., 2001; Guan & Wessel, 2022; Rey-Mermet & Meier, 2017a, 2017b; Ridderinkhof, 2002; Wessel, 2018). The shift occurs through increased response caution in the conflict monitoring system that affects the response criterion rather than delayed response onsets (Dutilh et al., 2012). Such a shift has been predicted by early computational simulations that act as a separate control mechanism from selective control (Botvinick et al., 2001: simulation 2C) as well as in a recent EEG study (Guan & Wessel, 2022). It is generally assumed that error and conflicts are correlated since errors are likely to occur in the presence of conflicts (e.g., Botvinick et al, 2001; Verguts et al., 2011), which suggests that post-conflict slowing also reflects a conservative shift in the response criterion. The shift can occur quickly within 300 ms of detecting a response conflict through a combination of bottom-up and top-down mechanisms (Wessel, 2018) and can last up to a few trials (Rey-Mermet & Meier, 2017a). Also, a common finding, including the current study, is that slowing triggered by conflict or errors occurs early in the next trial and occurs in a domain-general manner (Guan & Wessel, 2022; Rey-Mermet & Meier, 2017a, 2017b; Verguts et al., 2011; Wessel, 2018). Yet, it should be noted that there are other types of slowing effects that arise through different mechanisms, such as the bivalency effect in task switching, sustained response slowing due to proportion differences in conflict trials between blocks (see Rey-Mermet & Meier, 2017a, 2017b for a thorough investigation), or difficulty related slowing effects (Taylor & Lupker, 2001). This implies that the mechanism of sequential slowing effects may be task dependent, which is a good topic for future investigations (also see Schmidt & Weissman, 2014; Spinelli & Lupker, 2022 for relevant discussions).

4.7. Slow-and-suppress in s-r mapping conflicts

Considering our findings showing post-conflict slowing in movement speed dynamics and the CSE in spatial dynamics, we propose a *slow-and-suppress* account of the CSE for the Simon task and spatial versions of conflict tasks (e.g., arrow flankers). In this account, response conflict is continuously monitored, and automatic task-irrelevant activations are suppressed on N^0 incongruent trials. Experiencing response conflicts or making a response error prepares participants for subsequent trials by adjusting the speed-accuracy response criterion. This adjustment results in a general slowing of responses on the following trial(s) but also improves the precision of movement. When response conflict repeats on a subsequent incongruent trial, suppression intensifies, leading to improved performance. The question of whether different conflict tasks engage distinct control mechanisms is still under investigation and requires further extensive research. Presumably *slow-and-amplify* may be more suitable for tasks without spatial conflicts such as in the typical Stroop task.

4.8. Can repetition priming skip a trial?

Even in the confound-minimized alternating design, repetition priming confounds from N^{-2} trials can have lingering effects on the sequential modulations (Erb & Aschenbrenner, 2019; Lim & Cho, 2021a). To test the extent of lingering priming effects, Lim and Cho (2021a) reanalyzed one cross-task Simon and three cross-task flanker experiments from two previous studies (Lim & Cho, 2018, 2021b) and concluded that repetition priming from N^{-2} trials does occur but has minimal impact on the CSE. They demonstrated that the pattern of CSE from repetition priming and the pattern of from cognitive control are similar after *congruency* repetitions between N^{-2} and N^{-1} trials, but the pattern is opposite after congruency switches minimizing the CSE. When considering the entire dataset, the sequential modulation from cognitive control remains unaffected while the modulation from repetition priming largely cancels out.

Lim and Cho (2021a) further showed that the CSE shrinkage after congruency switches only occurs when responses between alternating tasks share a common response mode (e.g. same vs. different hands) or when the alternating stimuli evokes spatial conflicts due to common S-R mapping rules (e.g., alphabetical order of letters, arrow stimuli). This ruled out the alternative multiple expectancy account (Erb & Aschenbrenner, 2019) which explains that sequential modulations occur through top-down predictions about upcoming response conflicts based on congruency repetitions from a sequence preceding trial.

Our experimental design is almost identical to the same response mode condition from Lim and Cho's (2021b) Experiment 1. Consistent with the re-analysis, nearly all measurements showed pronounced CSEs after congruency repetitions that diminished after switches. We also directly showed that feature repetition between N^{-2} trials and N^0 trials does not facilitate responses, showing that repetition priming exerts a minimum amount of influence within the current experimental design. We have not tested our results using cross-task alternations with different response modes but based on the re-analysis we conclude that repetition priming had a minimal effect and that the sequential modulations in the current dataset can be attributed to cognitive control.

4.9. Post-congruence facilitation

Before concluding the study, there are a couple of issues that are worth considering in future investigations. First is whether the post-conflict slowing effects in the current and previous studies are in part due to post-congruence facilitation and whether the selective control mechanism is due to increased or decreased control. For example, Compton, Huber, Levinson, and Zheutlin (2012) showed that the CSE is dramatically smaller (larger interference) after congruent trials than after incongruent or neutral trials, indicating that decreased control drives the CSE. In contrast, Aisenberg and Henik (2012), introduced neutral conditions in a Simon task and showed that the Simon effect after neutral trials were similar to congruent trials and that the CSE was driven by increased control. A recent diffusion modelling study also provides evidence that the effects of congruent trials are small or even non-existent in flanker and Simon tasks (Evans & Servant, 2022). Meanwhile, Treccani, Cona, Milanese, and Umiltà (2018) observed both signs of increased and decreased control. These studies differed in how repetition priming was handled, suggesting that adding a neutral condition to a confound-minimized Simon task and in other tasks is a promising topic for future investigation.

4.10. On movement procedures

Another consideration is the different response limits adopted across studies, which have ranged from 1 to 3 s. A more lenient response limit can delay the onset of an overt response, but sufficiently fast response onsets are required for cognitive processes to be reflected in behavioral responses (Chen & Johnson, 1991; Hehman et al., 2015). Several procedural recommendations exist to ensure sufficiently fast mouse movement responses. Perhaps the most common way is to set a reasonable maximum response limit, emphasize the need for *fast and accurate* responses, and provide feedback (e.g., Dieciuc et al., 2019; Erb et al., 2016; Erb et al., 2019; Erb & Marcovitch, 2019; Moher, Anderson, & Song, 2015). In this regard, a narrower response window may promote faster response initiations. A more advanced method would be to introduce a response onset cutoff in addition to a maximum response limit (e.g., Hehman et al., 2015; Kim, 2024). A general recommendation is around 400 ms, but applying a uniform onset cutoff requires prior knowledge about the task difficulty and the minimum processing time required (Hehman et al., 2015). Another effective way is to dynamically initiate a trial by presenting the stimulus display upon initiating a mouse movement (e.g., Scherbaum et al., 2018; Scherbaum & Dschemuchadse, 2010; Scherbaum & Kieslich, 2018). For example, Scherbaum and Kieslich (2018) demonstrated dynamic trial initiation improves the statistical power of sequential modulations in a SNARC congruency task. Finally, an effective alternative would be to use a diametrically opposite response layout rather than using a layout that place stimuli and response boxes on the same side of the screen. The diametric layout is known to increase the cost of movement in the wrong direction which leads to better movements measurements (Buetti & Kerzel, 2008; Wirth et al., 2020).

5. Conclusion

The present study employed computer mouse tracking to uncover the mechanisms underlying the sequential modulation of cognitive control enhanced by past response conflict using the Simon task. By employing an experimental design that minimizes the influence of repetition priming, contingency learning, and error-related control, we observed novel findings indicating that post-conflict slowing and congruence sequence effects are differentially represented in the spatiotemporal dynamics of movement speed and direction. Furthermore, these findings suggest that general post-conflict slowing contributes to the congruency sequence effect in joint with selective control of task-irrelevant response activations. This broadly implies that the human cognitive system can utilize multiple control mechanisms to optimize performance in response to increased performance demands.

Funding

This research was supported by the Korean Research Foundation Grant funded by the Korean Government (NRF-2020R1A2C2012033) and a faculty research grant from the School of Psychology at Korea University in 2024. Correspondence concerning this paper should be addressed to Yang Seok Cho, School of Psychology, Korea University, 145 Anam-ro, Seongbuk-gu, Seoul, Korea, 02841. *E*-mail: yscho_psych@korea.ac.kr. The corresponding datasets are available at the Open Science Framework: https://osf.io/5vpuw/

Declaration of generative AI and AI-assisted technologies in the writing process

During the preparation of this work, the author(s) used GPT-4o mini was used for final proof-reading purposes for some parts of this manuscript (OpenAI, 2023). After using this tool/service, the authors reviewed and edited the content as needed and took full responsibility for the content of the published article.

CRediT authorship contribution statement

Minwoo J.B. Kim: Writing – review & editing, Writing – original draft, Visualization, Methodology, Formal analysis, Data curation. **Chae Eun Lim:** Writing – original draft, Formal analysis, Data curation, Conceptualization. **Hansol Rheem:** Writing – original draft, Visualization, Formal analysis, Conceptualization. **Nahyun Lee:** Writing – original draft, Visualization, Formal analysis. **Yang Seok Cho:** Writing – review & editing, Project administration, Funding acquisition, Conceptualization.

Declaration of competing interest

Authors declare no conflict of interest.

Data availability

The corresponding datasets are available at the Open Science Framework: https://osf.io/5vpuw/.

References

Aisenberg, D., & Henik, A. (2012). Stop being neutral: Simon takes control! *Quarterly Journal of Experimental Psychology, 65*(2), 295–304.

Botvinick, M. M., Braver, T. S., Barch, D. M., Carter, C. S., & Cohen, J. D. (2001). Conflict monitoring and cognitive control. *Psychological Review, 108*(3), 624–652.

Braem, S., Abrahamse, E. L., Duthoo, W., & Notebaert, W. (2014). What determines the specificity of conflict adaptation? A review, critical analysis, and proposed synthesis. *Frontiers in Psychology, 5*, 1134.

Buetti, S., & Kerzel, D. (2008). Time course of the Simon effect in pointing movements for horizontal, vertical, and acoustic stimuli: Evidence for a common mechanism. *Acta Psychologica, 129*(3), 420–428.

Buetti, S., & Kerzel, D. (2009). Conflicts during response selection affect response programming: Reactions towards the source of stimulation. *Journal of Experimental Psychology: Human Perception and Performance, 35*(3), 816–834.

Calderon, C. B., Gevers, W., & Verguts, T. (2018). The unfolding action model of initiation times, movement times, and movement paths. *Psychological Review, 125*(5), 785–805.

Campbell, J. I., & Thompson, V. A. (2012). MorePower 6.0 for ANOVA with relational confidence intervals and Bayesian analysis. *Behavior Research Methods, 44*, 1255–1265.

Chen, J. Y., & Johnson, M. K. (1991). The Stroop congruency effect is more observable under a speed strategy than an accuracy strategy. *Perceptual and Motor Skills, 73*(1), 67–76.

Compton, R. J., Huber, E., Levinson, A. R., & Zheutlin, A. (2012). Is "conflict adaptation" driven by conflict? Behavioral and EEG evidence for the underappreciated role of congruent trials. *Psychophysiology, 49*(5), 583–589.

Dale, R., Kehoe, C., & Spivey, M. J. (2007). Graded motor responses in the time course of categorizing atypical exemplars. *Memory & Cognition, 35*(1), 15–28.

De Jong, R., Liang, C.-C., & Lauber, E. (1994). Conditional and unconditional automaticity: A dual-process model of effects of spatial stimulus-response correspondence. *Journal of Experimental Psychology: Human Perception and Performance, 20*(4), 731–750.
Dieciuc, M. A., Roque, N. A., & Boot, W. R. (2019). The spatial dynamics of mouse-tracking reveal that attention capture is stimulus-driven rather than contingent upon top-down goals. *Journal of Experimental Psychology: Human Perception and Performance, 45*(10), 1285–1290.
Dutilh, G., Vandekerckhove, J., Forstmann, B. U., Keuleers, E., Brysbaert, M., & Wagenmakers, E. J. (2012). Testing theories of post-error slowing. *Attention, Perception, & Psychophysics, 74*, 454–465.
Egner, T. (2008). Multiple conflict-driven control mechanisms in the human brain. *Trends in Cognitive Sciences, 12*(10), 374–380.
Egner, T. (2014). Creatures of habit (and control): A multi-level learning perspective on the modulation of congruency effects. *Frontiers in Psychology, 5*, 1247.
Egner, T., & Hirsch, J. (2005). Cognitive control mechanisms resolve conflict through cortical amplification of task-relevant information. *Nature Neuroscience, 8*, 1784–1790.
Erb, C. D., & Aschenbrenner, A. J. (2019). Multiple expectancies underlie the congruency sequence effect in confound-minimized tasks. *Acta Psychologica, 198*, Article 102869.
Erb, C. D., & Marcovitch, S. (2018). Deconstructing the Gratton effect: Targeting dissociable trial sequence effects in children, pre-adolescents, and adults. *Cognition, 179*, 150–162.
Erb, C. D., & Marcovitch, S. (2019). Tracking the within-trial, cross-trial, and developmental dynamics of cognitive control: Evidence from the Simon task. *Child Development, 90*(6), e831–e848.
Erb, C. D., McBride, A. G., & Marcovitch, S. (2019). Associative priming and conflict differentially affect two processes underlying cognitive control: Evidence from reaching behavior. *Psychonomic Bulletin & Review, 26*, 1400–1410.
Erb, C. D., Moher, J., Sobel, D. M., & Song, J. H. (2016). Reach tracking reveals dissociable processes underlying cognitive control. *Cognition, 152*, 114–126.
Erb, C. D., Smith, K. A., & Moher, J. (2021). Tracking continuities in the flanker task: From continuous flow to movement trajectories. *Attention, Perception, & Psychophysics, 83*, 731–747.
Erb, C. D., Welhaf, M. S., Smeekens, B. A., Moreau, D., Kane, M. J., & Marcovitch, S. (2021). Linking the dynamics of cognitive control to individual differences in working memory capacity: Evidence from reaching behavior. *Journal of Experimental Psychology: Learning, Memory, and Cognition, 47*(9), 1383.
Eriksen, B. A., & Eriksen, C. W. (1974). Effects of noise letters upon the identification of a target letter in a nonsearch task. *Perception & Psychophysics, 16*, 143–149.
Evans, N. J., & Servant, M. (2022). A model-based approach to disentangling facilitation and interference effects in conflict tasks. *Psychological Review, 129*(5), 1183.
Finkbeiner, M., & Heathcote, A. (2016). Distinguishing the time- and magnitude-difference accounts of the Simon effect: Evidence from the reach-to-touch paradigm. *Attention, Perception, & Psychophysics, 78*, 848–867.
Gratton, G., Coles, M. G., & Donchin, E. (1992). Optimizing the use of information: Strategic control of activation of responses. *Journal of Experimental Psychology: General, 121*(4), 480–506.
Guan, Y., & Wessel, J. R. (2022). Two types of motor inhibition after action errors in humans. *Journal of Neuroscience, 42*(38), 7267–7275.
Hehman, E., Stolier, R. M., & Freeman, J. B. (2015). Advanced mouse-tracking analytic techniques for enhancing psychological science. *Group Processes & Intergroup Relations, 18*(3), 384–401.
Heuer, H., & Wühr, P. (2025). The functional role of the task-irrelevant stimulus feature in the congruency sequence effect. *Journal of Experimental Psychology: Learning, Memory, and Cognition, 51*(5), 704–736.
Hommel, B. (1994). Spontaneous decay of response-code activation. *Psychological Research, 56*(4), 261–268.
Hommel, B., Müsseler, J., Aschersleben, G., & Prinz, W. (2001). The theory of event coding (TEC): A framework for perception and action planning. *Behavioral and Brain Sciences, 24*(5), 849–878.
Hommel, B., Proctor, R. W., & Vu, K. P. L. (2004). A feature-integration account of sequential effects in the Simon task. *Psychological Research, 68*, 1–17.
Hübner, R., & Mishra, S. (2013). Evidence for strategic suppression of irrelevant activation in the Simon task. *Acta Psychologica, 144*(1), 166–172.
Hübner, R., & Töbel, L. (2019). Conflict resolution in the Eriksen flanker task: Similarities and differences to the Simon task. *PLoS One, 14*(3), Article e0214203.
JASP Team. (2024). *JASP (Version 0.18.2.0)[Computer software]*.
Kieslich, P. J., & Henninger, F. (2017). Mousetrap: An integrated, open-source mouse-tracking package. *Behavior Research Methods, 49*, 1652–1667.
Kim, M. J. (2024). Emotional capture of spatial attention is suppressed in high anxiety but at a non-spatial time cost. *Visual Cognition, 32*(2), 97–114.
Kim, S., & Cho, Y. S. (2014). CSE without feature integration and contingency learning. *Acta Psychologica, 149*(1), 60–68.
Kim, S., Lee, S. H., & Cho, Y. S. (2015). Control processes through the suppression of the automatic response activation triggered by task-irrelevant information in the Simon-type tasks. *Acta Psychologica, 162*(1), 51–61.
King, J. A., Korb, F. M., von Cramon, D. Y., & Ullsperger, M. (2010). Post-error behavioral adjustments are facilitated by activation and suppression of task-relevant and task-irrelevant information processing. *Journal of Neuroscience, 30*(38), 12759–12769.
Lee, J., & Cho, Y. S. (2013). CSE in cross-task context: Evidence for dimension-specific modulation. *Acta Psychologica, 144*(3), 617–627.
Lee, N., & Cho, Y. S. (2024). Investigating the nature of spatial codes for different modes of Simon tasks: Evidence from congruency sequence effects and delta functions. *Journal of Experimental Psychology: Human Perception and Performance, 50*(8), 819–841.
Lee, P. S., & Sewell, D. K. (2024). A revised diffusion model for conflict tasks. *Psychonomic Bulletin & Review, 31*(1), 1–31.
Lee, Y. S., Bae, G. Y., & Cho, Y. S. (2025). Inhibition resolves Simon conflict: Evidence from electroencephalogram decoding. *Journal of Cognitive Neuroscience, 1-21*. https://doi.org/10.1162/jocn.a.59
Lee, Y. S., & Cho, Y. S. (2023). The congruency sequence effect of the Simon task in a cross-modality context. *Journal of Experimental Psychology: Human Perception and Performance, 49*(9), 1221–1235.
Lim, C. E., & Cho, Y. S. (2018). Determining the scope of control underlying the congruency sequence effect: Roles of stimulus-response mapping and response mode. *Acta Psychologica, 190*, 267–276.
Lim, C. E., & Cho, Y. S. (2021a). Cross-task congruency sequence effect without the contribution of multiple expectancy. *Acta Psychologica, 214*, Article 103268.
Lim, C. E., & Cho, Y. S. (2021b). Response mode modulates the congruency sequence effect in spatial conflict tasks: Evidence from aimed-movement responses. *Psychological Research, 85*(5), 2047–2068.
Luo, C., & Proctor, R. W. (2022). A diffusion model for the congruency sequence effect. *Psychonomic Bulletin & Review, 29*(6), 2034–2051.
Mathôt, S., Schreij, D., & Theeuwes, J. (2012). OpenSesame: An open-source, graphical experiment builder for the social sciences. *Behavior Research Methods, 44*, 314–324.
Mayr, U., Awh, E., & Laurey, P. (2003). Conflict adaptation effects in the absence of executive control. *Nature Neuroscience, 6*(5), 450–452.
Miller, J., & Schwarz, W. (2021). Delta plots for conflict tasks: An activation-suppression race model. *Psychonomic Bulletin & Review*, 1–20.
Mittelstädt, V., Leuthold, H., & Mackenzie, I. G. (2023). Motor demands influence conflict processing in a mouse-tracking Simon task. *Psychological Research, 87*(6), 1768–1783.
Mittelstädt, V., Miller, J., Leuthold, H., Mackenzie, I. G., & Ulrich, R. (2022). The time-course of distractor-based activation modulates effects of speed-accuracy tradeoffs in conflict tasks. *Psychonomic Bulletin & Review, 29*(3), 837–854.
Moher, J., Anderson, B. A., & Song, J. H. (2015). Dissociable effects of salience on attention and goal-directed action. *Current Biology, 25*(15), 2040–2046.
Mordkoff, J. T. (2012). Observation: Three reasons to avoid having half of the trials be congruent in a four-alternative forced-choice experiment on sequential modulation. *Psychonomic Bulletin & Review, 19*, 750–757.
Nosek, B. A., Alter, G., Banks, G. C., Borsboom, D., Bowman, S. D., Breckler, S. J., … Yarkoni, T. (2015). Scientific standards: Promoting an open research culture. *Science, 348*(6242), 1422–1425. https://doi.org/10.1126/science.aab2374
Notebaert, W., Gevers, W., Verbruggen, F., & Liefooghe, B. (2006). Top-down and bottom-up sequential modulations of congruency effects. *Psychonomic Bulletin & Review, 13*(1), 112–117.
OpenAI. (2023). *GPT-4o mini [Large language model]*. https://chatgpt.com.
Proctor, R. W., & Cho, Y. S. (2006). Polarity correspondence: A general principle for performance of speeded binary classification tasks. *Psychological Bulletin, 132*(3), 416–442.
Rey-Mermet, A., & Meier, B. (2017a). How long-lasting is the post-conflict slowing after incongruent trials? Evidence from the Stroop, Simon, and flanker tasks. *Attention, Perception, & Psychophysics, 79*, 1945–1967.
Rey-Mermet, A., & Meier, B. (2017b). Post-conflict slowing after incongruent stimuli: From general to conflict-specific. *Psychological Research, 81*, 611–628.
Rheem, H., Vaughn Becker, D., & Craig, S. D. (2021). Assessing learning effort with hand motion tracking methods. *Applied Cognitive Psychology, 35*(3), 606–620.
Ridderinkhof, R. K. (2002). Micro-and macro-adjustments of task set: Activation and suppression in conflict tasks. *Psychological Research, 66*(4), 312–323.
Salzer, Y., & Friedman, J. (2020). Reaching trajectories unravel modality-dependent temporal dynamics of the automatic process in the Simon task: A model-based approach. *Psychological Research, 84*, 1700–1713.
Scherbaum, S., Dshemuchadse, M., Fischer, R., & Goschke, T. (2010). How decisions evolve: The temporal dynamics of action selection. *Cognition, 115*, 407–416.
Scherbaum, S., Dshemuchadse, M., & Kalis, A. (2008). Making decisions with a continuous mind. *Cognitive, Affective, & Behavioral Neuroscience, 8*, 454–474.
Scherbaum, S., Frisch, S., Dshemuchadse, M., Rudolf, M., & Fischer, R. (2018). The test of both worlds: Identifying feature binding and control processes in congruency sequence tasks by means of action dynamics. *Psychological Research, 82*, 337–352.
Scherbaum, S., & Kieslich, P. J. (2018). Stuck at the starting line: How the starting procedure influences mouse-tracking data. *Behavior Research Methods, 50*, 2097–2110.
Schmidt, J. R., & De Houwer, J. (2011). Now you see it, now you don't: Controlling for contingencies and stimulus repetitions eliminates the Gratton effect. *Acta Psychologica, 138*(1), 176–186.
Schmidt, J. R., & Weissman, D. H. (2014). Congruency sequence effects without feature integration or contingency learning confounds. *PLoS One, 9*(7), Article e102337.
Simon, J. R., & Rudell, A. P. (1967). Auditory S-R compatibility: The effect of an irrelevant cue on information processing. *Journal of Applied Psychology, 51*(3), 300–304.
Song, J. H., & Nakayama, K. (2009). Hidden cognitive states revealed in choice reaching tasks. *Trends in Cognitive Sciences, 13*(8), 360–366.
Soutschek, A., Müller, H. J., & Schubert, T. (2013). Conflict-specific effects of accessory stimuli on cognitive control in the Stroop task and the Simon task. *Experimental Psychology, 60*(2), 140–148.
Spinelli, G., & Lupker, S. J. (2022). Conflict-monitoring theory in overtime: Is temporal learning a viable explanation for the congruency sequence effect? *Journal of Experimental Psychology: Human Perception and Performance, 48*(5), 497.

Spivey, M. J., Grosjean, M., & Knoblich, G. (2005). Continuous attraction toward phonological competitors. *Proceedings of the National Academy of Sciences, 102*(29), 10393–10398.

Stroop, J. R. (1935). Studies of interference in serial verbal reactions. *Journal of Experimental Psychology, 18*(6), 643–662.

Stürmer, B., & Leuthold, H. (2003). Control over response priming in visuomotor processing: A lateralized event-related potential study. *Experimental Brain Research, 153*, 35–44.

Stürmer, B., Leuthold, H., Soetens, E., Schröter, H., & Sommer, W. (2002). Control over location-based response activation in the Simon task: Behavioral and electrophysiological evidence. *Journal of Experimental Psychology: Human Perception and Performance, 28*(6), 1345–1363.

Taylor, T. E., & Lupker, S. J. (2001). Sequential effects in naming: A time-criterion account. *Journal of Experimental Psychology: Learning, Memory, and Cognition, 27*(1), 117.

Treccani, B., Cona, G., Milanese, N., & Umiltà, C. (2018). Sequential modulation of (bottom–up) response activation and inhibition in a response conflict task: A single-pulse transcranial magnetic stimulation study. *Psychological Research, 82*, 771–786.

van Rossum, G. (1995). Centrum voor Wiskunde en Informatica. *Centrum voor Wiskunde en Informatica. Python tutorial. Technical Report CS-R9526. Amsterdam*.

Van den Bergh, D., Wagenmakers, E. J., & Aust, F. (2023). Bayesian repeated-measures analysis of variance: An updated methodology implemented in JASP. *Advances in Methods and Practices in Psychological Science, 6*(2), 25152459231168024.

Verguts, T., Notebaert, W., Kunde, W., & Wühr, P. (2011). Post-conflict slowing: Cognitive adaptation after conflict processing. *Psychonomic Bulletin & Review, 18*(1), 76–82.

Welsh, T. N., & Elliott, D. (2004). Movement trajectories in the presence of a distracting stimulus: Evidence for a response activation model of selective reaching. *The Quarterly Journal of Experimental Psychology, 57*, 1031–1057.

Wessel, J. R. (2018). An adaptive orienting theory of error processing. *Psychophysiology, 55*(3), Article e13041.

Wirth, R., Foerster, A., Kunde, W., & Pfister, R. (2020). Design choices: Empirical recommendations for designing two-dimensional finger-tracking experiments. *Behavior Research Methods, 52*, 2394–2416.